Mon. Not. R. Astron. Soc. **000**, 1–11 (2017) Printed 12 June 2019 (MN LATEX style file v2.2)

Targeted search for young radio pulsars in the SMC: Discovery of two new pulsars

N. Titus[1,2⋆], B. W. Stappers[3], V. Morello[3], M. Caleb[3,4,5,6], M. D. Filipović[7], V. A. McBride[1,2,8], W. C. G. Ho[9,10] D. A. H. Buckley[2]
[1]*Department of Astronomy, University of Cape Town, Private Bag X3, Rondebosch, 7701, South Africa*
[2]*South African Astronomical Observatory, PO Box 9, Observatory, 7935, South Africa*
[3]*Jodrell Bank Centre for Astrophysics, School of Physics and Astronomy, University of Manchester, Manchester M13 9PL, UK*
[4]*Research School of Astronomy and Astrophysics, Australian National University, ACT, 2611, Australia*
[5]*Centre for Astrophysics and Supercomputing, Swinburne University of Technology, P.O. Box 218, Hawthorn, VIC 3122, Australia*
[6]*ARC Centre of Excellence for All-sky Astrophysics (CAASTRO)*
[7]*Western Sydney University, Locked Bag 1797, Penrith South DC, NSW 1797, Australia*
[8]*IAU Office of Astronomy for Development, Cape Town, South Africa*
[9]*Department of Physics and Astronomy, Haverford College, 370 Lancaster Avenue, Haverford, PA 19041 USA*
[10]*Mathematical Sciences, Physics and Astronomy and STAG Research Centre, University of Southampton, SO17 1BJ, UK*

Accepted 2019 June 4. Received 2019 June 4; in original form 2019 April 17

ABSTRACT
We report the first rotation powered pulsars discovered in the Small Magellanic Cloud (SMC) in more than a decade. PSR J0043–73 and PSR J0052–72 were discovered during a Parkes Multi-Beam (PMB) survey of MCSNR J0127-7332, and five new, optically selected, supernova remnant (SNR) candidates identified by the XMM Newton survey. In addition to the candidates, we adjusted the PMB rotation to include an additional nine SNRs and pulsar wind nebulae. We searched for young pulsars (1 – 200 ms) employing a Fourier analysis with `PRESTO`, as well as a search for longer period pulsars (200 ms – 360 s) with a fast folding algorithm. Our targeted survey had a limiting flux density of 0.039 mJy for periods greater than 50 ms. Although not the main target of this search it was also sensitive to millisecond pulsars. PSR J0043–73 has a period and dispersion measure of 937.42937 (26) ms and 115.1 (3.4) pc cm^{-3} respectively, and PSR J0052–72 has a period of 191.444328 (46) ms and a DM of 158.6 (1.6) pc cm^{-3}.

Key words: pulsars: general – supernova remnants – Magellanic Clouds

1 INTRODUCTION

The Magellanic Clouds (MCs) are our closest satellite galaxies, and the only galaxies other than the Milky Way in which we have been able to detect radio pulsars. The MCs have gone through a relatively recent episode of star formation (Antoniou & Zezas 2016), producing a large number of O and B stars, many of which are companions in high mass X-ray binary (HMXB) systems. A recent census (Haberl & Sturm 2015) identified 120 HMXBs (of which 63 are X-ray pulsars) in the Small Magellanic Cloud (SMC) – similar to the population in the Milky Way, despite the fact that the SMC is only one-fiftieth the mass. This is a clear indication that the SMC harbours many neutron stars (NSs) and many in interesting binaries. However, despite this large population of NSs only five rotation powered pulsars so far have been discovered in the SMC through various MC radio surveys (McConnell et al. 1991; Crawford et al. 2001; Manchester et al. 2006).

Massive stars form NSs during core-collapse supernova events. Most of the newly formed NSs are rotation-powered pulsars (Keane & Kramer 2008), which emit pulsed, non-thermal radio emission. Energetic young radio pulsars can produce an outflow of relativistic particles which will interact with their natal SNR and the surrounding interstellar medium, creating a pulsar wind nebula (PWN). Thus, SNRS and PWNe are excellent candidates for targeted radio pulsar surveys, that being said pulsars have so far only been discovered in ~50% of SNRs and PWNe (Green 2014). The lack of SNRs and PWNe associations with pulsars may be the result of beaming effects, or alternatively due to instrumentation sensitivity limits. Camilo (2003) completed a census of SNR-pulsar associations (Kaspi, V. M., Helfand 2002; Gorham et al. 1996; Lorimer et al. 2000; Manchester et al. 2001) and found that in some cases the pulsars asso-

⋆ E-mail: naomi@saao.ac.za

ciated with SNRs can be faint. Hence, deep surveys may be required to detect these young radio pulsars.

The first of the SMC surveys using the Parkes radio telescope was conducted by McConnell et al. (1991) with a limiting mean flux density at 610 MHz of 0.5 - 0.8 mJy for pulsars with periods greater than 500 ms and dispersion measure (DMs) of 100 pc cm^{-3} or less. The survey discovered 1 pulsar, PSR J0045–7319, later shown to be in a 51 day orbit around a 16$^{\rm th}$ magnitude B star (Kaspi et al. 1994). In a subsequent SMC survey with the 20 cm Multi-Beam receiver at Parkes (PMB), Crawford et al. (2001) discovered PSR J0113–7220. The survey covered a more complete region of the SMC (~6.7 deg^2) with a limiting flux density of 0.08 mJy at 1400 MHz for pulsars with periods greater than 50 ms and DMs less than 200 pc cm^{-3}. The most recent and successful SMC survey was conducted by Manchester et al. (2006), also using the PMB receiver, in which three pulsars were detected (PSR J0045–7042, PSR J0111–7131, PSR J0131–7310). The advantage of the Manchester et al. (2006) survey was the increased DM range of up to 277 pc cm^{-3}, however it was most sensitive to periods greater than 50 ms, but with a similar limiting flux density to the Crawford et al. (2001) survey.

Due to the distance to the SMC (~60 kpc), the blind surveys only detected the brightest pulsars, since integration time is sacrificed to cover a larger area. To improve upon the sensitivity of the previous blind surveys we carried out the deepest, most sensitive pulsar searches of five supernova remnant (SNR) candidates, as well as MCSNR J0127-7332 in the SMC. Finding a young pulsar which is coincident with its natal SNR or within a PWN will enable studies of the initial spin period, velocity, and magnetic field distributions of young NSs, providing insights to the physics governing core-collapse. It also enable searches at other energies, particularly X-ray observations can facilitate NS cooling studies. Finding just one new pulsar in the SMC will provide valuable details about the nature of the SMC pulsar population and the progenitor stars that formed it. Particularly, the low metallicity environment of the SMC will affect mass loss of massive stars uniquely when compared to the Galaxy. This may be reflected in the distribution of angular momentum of the radio pulsars.

In this paper we present the results for our targeted pulsar searches in the SMC. In Section 2, we describe the observations, followed by the data reduction process in Section 3. In Section 4 we present the results, and discuss their implications in Section 5. Finally, in Section 6, we draw our conclusions.

2 SOURCE SELECTION AND OBSERVATIONS

2.1 Supernova Remnant Candidates

The XMM-Newton satellite has conducted the deepest complete survey of the SMC in the 0.15–12.0 keV X-ray band to date (Haberl et al. 2012; Sturm et al. 2013). The relatively close and known distance to the SMC (60 kpc) together with the moderate Galactic foreground absorption of NH $\approx 6{\times}10^{20}$ cm^{-2} (Dickey & Lockman 1990) provides an opportunity to study the complete X-ray source population within the SMC. These are dominated by HXMBs, SNRs and super-soft X-ray sources. In total the survey detected 23 SNRs, 20 previously known (Badenes et al. 2010) and 3 new candidates, XMMU J0049-7306, XMMU J0056.6-7208 and XMMU J0057.7-7213.

Following a study of narrow band optical images (Hα and SII) and ATCA radio observations (Filipović et al. 2005; Payne et al. 2007, Roper et al. 2015; Maggi et al. 2019, submitted) of the SMC, nine new SNR candidates were selected for further study. One of these (SNR C1) was found to be coincident with one of the newly identified XMM-Newton SNRs (Haberl et al. 2012), namely XMMU J0056.6-7208. Following SALT long slit spectroscopy of 8 of these new candidate SNRs, SII/Hα ratios were determined and indicated that 6 were consistent with being SNR. These, plus the two other XMM-Newton SNR candidates were then selected to be observed by SALT using the Fabry-Perot imaging at Hα, SII and OIII. In the end only 7 SNRs candidates were observed, of which 4 showed strong evidence for SNR shells, namely SNR C1 (=XMMU J0056.6-7208), SNR C3, SNR C4 & SNR C9). The 3 others showed either indistinct or small shells (SNR C2, SNR C6 & XMMU J0057.7-7213). A known SNR, MCSNR J0127-7332, which is associated with a slowly spinning X-ray pulsar SXP 1062 in a Be X-ray binary (Hénault-Brunet et al. 2012), was observed as a control object, which was confirmed as a SNR.

We were awarded 54 hours with the Parkes radio telescope to observe six of the SNR candidates (MCSNR J0127–7332, XMMU J0049.0–7306, SNR C3, SNR C2, XMMU J0056.6-7208, SNR C9), which were coincident with X-ray point sources.

Table 1. The PMB receiver properties as recorded by Manchester et al. (2001).

Beam	Centre	Inner	Outer
Gain (K Jy^{-1})	0.735	0.690	0.581
Half power beamwidth (arcmin)	14.0	14.1	14.5
Beam ellipticity	0.0	0.03	0.06
Coma lobe (dB)	none	17	14

2.2 Parkes Observations

The PMB receiver (Staveley-Smith et al. 1996) has the ability to observe 13 distinct regions on the sky similtaneously, covering a 0.5 deg^2 region, making it ideal for surveys. The PMB consists of the most sensitive central beam, six inner ring beams, and the six least sensitive outer ring beams. The beam properties are listed in Table 1.

We used the PMB with the Berkeley-Parkes-Swinburne data recorder (BPSR, McMahon 2008; Keith et al. 2010) to perform deep pulsar searches in the SMC. The focus of the survey was 5 optically selected SNR candidates, as well as a known SNR, MCSNR J0127-7332, which are coincident with X-ray point sources. The extent of the SNRs was less than the ~14 arcmin half power beam width (HPBW) of the PMB. The central beam of the PMB was positioned on the SNRs, and then rotated to include an additional 9 known SNRs and PWNe (Filipović et al. 2008). The targets are listed in Table 2. One beam of one pointing was adjusted as much as possible to the position of

PSR J0131–7310, a known radio pulsar in the SMC, with a period and DM of 348.124045581 (7) ms and 205.2 pc cm^{-3} respectively (Manchester et al. 2006). The PMB beam pattern and configuration is highlighted in Figure 1.

Our observations were carried out between 25 August 2017 and 13 December 2017, using a central frequency of 1382 MHz with a bandwidth of 400 MHz, split into 1024 channels, and a temporal resolution of 64 μs. Each field was observed twice (except for the MCSNR J0127-7332 pointing which was observed 3 times), separated on average by 20 days, with an integration time of ~15 000 s per pointing. This would allow us to cross match candidates identified in a pointing, as well as detect binary pulsars at a different orbital phase.

2.3 Survey Sensitivity

To compare our targeted survey with the previous blind surveys (Crawford et al. 2001; Manchester et al. 2006) we calculate the average, limiting flux density at 1400 MHz (S_{1400}) for each survey with the survey parameters recorded in Table 3. The average, fundamental limiting flux density for a survey is given by the radiometer equation

$$S_{lim} = \frac{\sigma \beta T_{sys}}{G\sqrt{n_p t_{int} \Delta\nu}}, \quad (1)$$

where the detection threshold, σ was chosen to be 8, and $\beta = 1.5$ for BPSR's 2-bit digitisation, which takes into account instrumental imperfections. For the PMB the mean system temperature is $T_{sys} = 23$ K (McMahon 2008; Keith et al. 2010), while the central PMB's gain is $G = 0.735$ K Jy^{-1}, with the number of polarisations, $n_p = 2$. The integration time (t_{int}) in seconds, and bandwidth ($\Delta\nu$) in MHz for the various surveys are recorded in Table 3. We used the same parameter values as outlined in Ridley et al. (2013) to calculate our sensitivity limits. The fundamental limiting flux density given by equation (1) for the Crawford et al. (2001) and Manchester et al. (2006) survey was 0.17 mJy, while our survey was more sensitive with a limiting flux density of 0.11 mJy.

These limits do not take into account the pulse width or broadening effects that must be accounted for, considering that a survey is not equally sensitive to all periods, pulse shapes, and DMs. We followed the methodology of Manchester et al. (2001) to model the frequency response of a pulsar. A series of pulses with frequency $f_p = 1/P$, where P is the pulse period, is portrayed in the Fourier domain by the fundamental and 8 harmonics. The respective harmonics have an amplitude of $1/S_{lim}$, which are multiplied by a sequence of functions representing the transformation the data will be subjected to. The first function accounts for the intrinsic pulse shape, which is modelled by a Gaussian with a width of $W_{50} = 0.05P$:

$$g_1(f_p) = exp\left(-\frac{\pi f_p {W_{50}}^2}{4ln2}\right). \quad (2)$$

The interstellar medium will then disperse the pulses, and cause a dispersion delay across a bandwidth of $\Delta\nu$, centred at a frequency of ν given by

$$\tau_{DM} = 8.3 \times 10^3 DM \Delta\nu \nu^{-3} s. \quad (3)$$

Thus, $g_2(f_p)$ is modelled by a similar Gaussian as in equation (2), but with W_{50} replaced with τ_{DM}. The final transformation has to account for the effect the finite sampling time (t_{samp}) has on the pulses, which is characterised by

$$g_3(f_p) = \left|\frac{sin(\pi f_p t_{samp})}{\pi f_p t_{samp}}\right|. \quad (4)$$

The final limiting sensitivity is given by summing over n harmonics, where $n \in \{1, 2, 4, 8\}$. Figure 2 shows the final limiting flux density for the various surveys at 1400 MHz for the average SMC DM of 116.4 pc cm^{-3}. It clearly shows our survey is the first to be sensitive to MSPs, and that for $P \geqslant 50$ ms our survey is twice as sensitive as the previous surveys. The respective flux densities for $P \geqslant 50$ ms are recorded in Table 3.

3 DATA REDUCTION

3.1 Young Pulsar Search

The PMB data were searched for young pulsars (i.e. those with periods of a few tens of milliseconds) using routines from `PRESTO`[1] (Ransom et al. 2002). Radio frequency interference (RFI) masks were created for each beam using `rfifind` with the `blocks` parameter set to 30. We searched 3 672 DMs within a range of 0 – 660 pc cm^{-3} (Table 4), with no restrictions on the period parameter space. The dedispersed time series was barycentred to correct for the Earth's motion and then Fourier transformed with `realfft`. The resulting power spectra were searched for significant pulses, which were summed up to the 8th harmonic using `accelsearch` with z = 0, i.e. no acceleration searches were conducted. Finally, candidates above a S/N threshold of 4.0 were selected and folded with `prepfold`. The low threshold was chosen, since we can cross-match candidates between pointings of the same field. We also observed PSR J0024-7204C at the start of every observing day, apart from the 2017–08–29 observations. The test pulsar was recovered with blind `PRESTO` searches at an expected S/N of 22, for every observation except on the 2017–09–11, when the observation was subjected to severe RFI.

The search identified ~150 000 candidates, which were are inspected by eye. Promising candidates were cross-checked with the alternate pointing of the same source on another day. If the candidate was not detected in the alternate pointing, the raw data was also folded with the identified period and DM.

3.2 Longer Period Pulsars

The Fast Fourier Transform method employed by PRESTO for the young pulsar search is susceptible to rednoise, which reduces the sensitivity for pulsars with periods greater than 200 ms (van Heerden et al. 2016). To combat the effects of rednoise we utilised a fast folding algorithm (FFA, Staelin

[1] https://www.cv.nrao.edu/ sransom/presto/

Table 2. Survey field observed in the SMC with the PMB.

Date	Target	Beam	Epoch[a] (MJD)	RA_{beam}[b] (J2000)	Dec_{beam}[b] (J2000)	t_{int}[c] (s)	Type (SNR/PWN)	Confirmed (yes/no)	Figure 1: PMB pattern
2017–08–25	MCSNR J0127-7332	1	57990.50	01 27 37.66	-73 35 20.50	16 223	SNR	yes	Red
	XMMU J0049.0-7306	1	57990.69	00 49 54.48	-73 04 09.70	12 989	SNR	no	Green
	DEM S5	13	57990.69	00 41 24.24	-73 39 24.80	12 989	PWN	yes	Green
	B0050-72.8	3	57990.69	00 51 35.18	-72 36 02.30	12 989	SNR	yes	Green
2017–08–28	SNR C3	1	57993.47	01 03 27.99	-72 03 41.30	16 217	SNR	no	Blue
	IKT 16	2[d]	57993.47	00 58 06.93	-72 19 17.60	16 217	PWN	yes	Blue
	IKT 21	1	57993.47	01 03 27.99	-72 03 41.30	16 217	SNR	yes	Blue
	1E0102-723	1	57993.47	01 03 27.99	-72 03 41.30	16 217	SNR	yes	Blue
	SNR C2	1	57993.66	00 56 31.02	-72 15 48.40	14 000	SNR	no	Cyan
	B0058-71.8	9	57993.66	01 00 19.47	-71 28 15.00	14 000	SNR	yes	Cyan
	IKT 25	10	57993.66	01 07 23.94	-72 06 41.50	14 000	SNR	yes	Cyan
2017–08–29	XMMU J0056.6-7208	1	57994.55	00 56 37.69	-72 09 01.40	16 223	SNR	no	Magenta
	N S66D	1	57994.55	00 56 37.69	-72 09 01.40	16 223	SNR	no	Magenta
	HFPK 334	12	57994.55	01 04 25.17	-72 45 33.80	16 223	SNR	yes	Magenta
	SNR C9	1	57994.74	01 12 39.07	-73 28 15.40	15 487	SNR	no	Yellow
2017–09–11[e]	MCSNR J0127-7332	1	58007.44	01 27 37.66	-73 35 20.50	16 224	SNR	yes	Red
	XMMU J0049.0-7306	1	58007.63	00 49 54.48	-73 04 09.70	12 319	SNR	no	Green
	DEM S5	13	58007.63	00 41 24.39	-73 39 25.40	12 319	PWN	yes	Green
	B0050-72.8	3	58007.63	00 51 35.18	-72 36 02.30	12 319	SNR	yes	Green
2017–09–12	SNR C3	1	58008.54	01 03 27.99	-72 03 41.30	16 221	SNR	no	Blue
	IKT 16	7[d]	58008.54	00 58 06.93	-72 19 17.60	16 221	PWN	yes	Blue
	IKT 21	1	58008.54	01 03 27.99	-72 03 41.30	16 221	SNR	yes	Blue
	1E0102-723	1	58008.54	01 03 27.99	-72 03 41.30	16 221	SNR	yes	Blue
	SNR C2[f]	1	58008.73	00 56 31.02	-72 15 48.40	5 436	SNR	no	Cyan
	B0058-71.8	9	58008.73	01 00 19.47	-71 28 15.00	5 436	SNR	yes	Cyan
	IKT 25	10	58008.73	01 07 23.94	-72 06 41.50	5 436	SNR	yes	Cyan
2017–09–28	XMMU J0056.6-7208	1	58024.52	00 56 37.69	-72 09 01.40	16 218	SNR	no	Magenta
	N S66D	1	58024.52	00 56 37.69	-72 09 01.40	16 218	SNR	no	Magenta
	HFPK 334	12	58024.52	01 04 25.26	-72 45 33.30	16 218	SNR	yes	Magenta
	SNR C9	1	58024.71	01 12 39.07	-73 28 15.40	13 469	SNR	no	Yellow
2017–12–13	MCSNR J0127-7332[g]	1	58100.47	01 27 37.66	-73 35 20.50	17 852	SNR	yes	Red

[a]The observation Epoch refers to the start of an observation.
[b]The PMB coordinates within which the SNR was located.
[c]t_{int} is the observation integration time.
[d]IKT 16: The PMB was rotated by 60°, resulting in a different beam number corresponding to the same beam coordinates. Thus on 2017–08–28 IKT 16 was located in beam 2, but in beam 7 on 2017–09–12.
[e]During the observations on 2017–09–11 strong RFI was detected.
[f]SNR C2: The observation was terminated due to strong winds.
[g]MCSNR J0127-7332: Additional Director's Time was allocated due to severe RFI during the 2017–09–11 pointing.

Table 3. Observational setup of SMC radio pulsar surveys, as well as the limiting flux densities at 1400 MHz for $P \geqslant 50$ ms. The flux densities were calculated as outlined in Section 2.3

Survey	Pointings	T_{int} (s)	t_{samp} (μs)	$\Delta\nu$ (MHz)	S_{1400} (mJy)
Crawford et al. (2001)	NA	8 400	250	288	0.066
Manchester et al. (2006)	73	8 400	1 000	288	0.067
This work	12	15 000	64	400	0.039

Table 4. Dedispersion parameters for young pulsar search.

Low DM (pc cm^{-3})	High DM (pc cm^{-3})	DM step (pc cm^{-3})	Down Sampling	Number DMs
0.00	196.80	0.10	1	1968
196.80	350.40	0.20	2	768
350.40	580.80	0.30	4	768
580.80	664.80	0.50	8	168

1969; Morelllo et al. 2019, in prep) to search for pulsars with periods from 200 ms − 360 s, and DMs from 0 − 400 pc cm^{-3} with DM steps of 2 pc cm^{-3}. The lower period limit was selected since the known pulsar distribution peaks at 200 ms, while the upper limit was the largest period we expect to have sufficient pulses to detect a pulsar. The data was dedispersed using `PRESTO`, while applying the same RFI masks created for the young pulsar search.

The FFA identified ~40 000 candidates, which were also inspected by eye. Acceptable candidates were cross matched with the alternate pointing in question, and folded with `PRESTO` using the period and DM identified by the FFA.

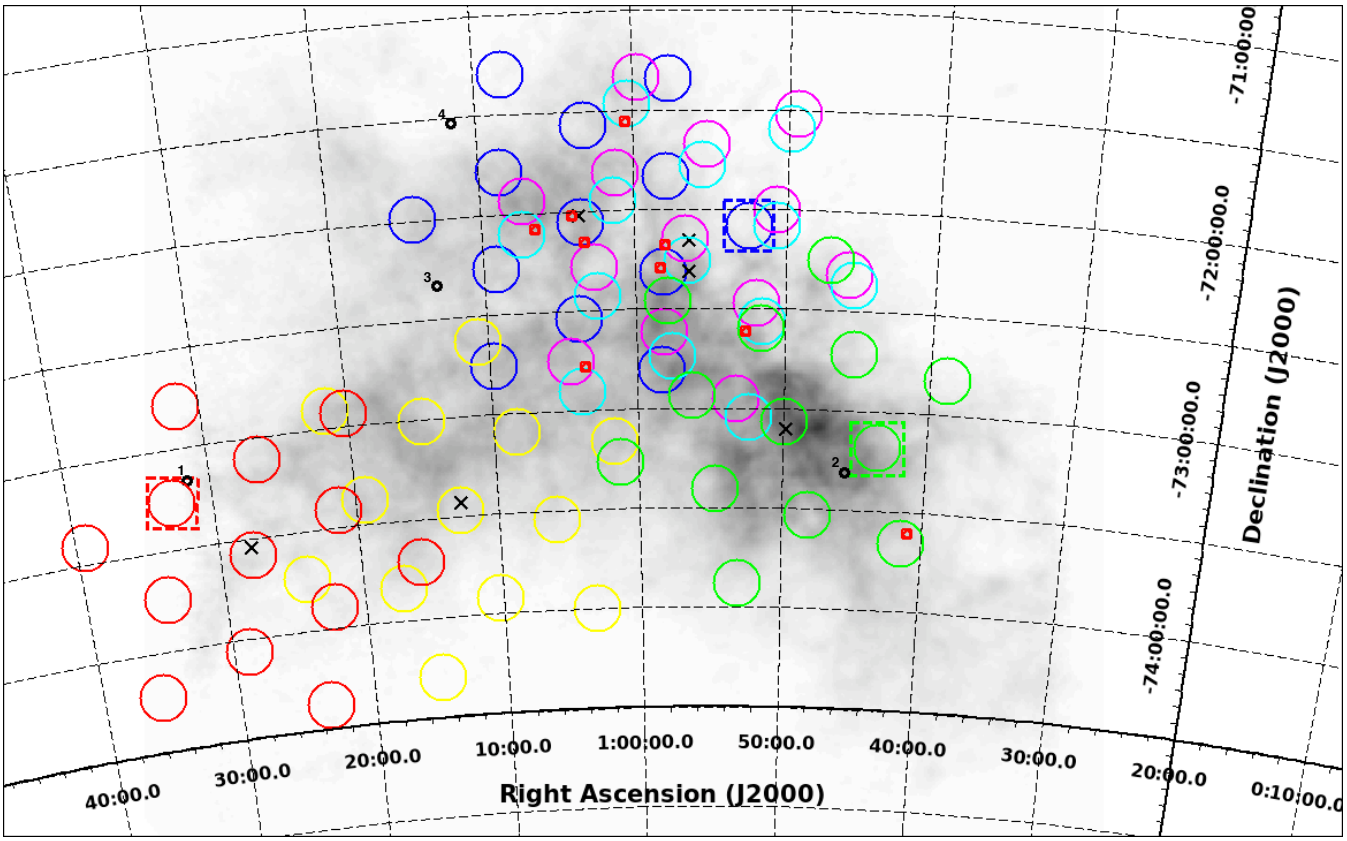

Figure 1. The coloured circles show the PMB orientation, where their 14 arcmin width is consistent with the half power beam width (HPBW) of the PMB beams (Table 1), and is superimposed on a HI map of the SMC (Stanimirovic et al. 1999). Furthermore, the locations of the five SNR candidates and MCSNR J0127-7332 are indicated by black crosses, and four of the known SMC radio pulsars are shown by black circles (1: PSR J0131–7310; 2: PSR J0045–7319; 3: PSR J0113–7220; 4: PSR J0111–7131; the fifth known pulsar is off the plot on the right hand corner). The nine additional SNRs and PWNe are highligted with small red squares. The dashed squares indicate the beams within which pulsars were detected: PSR J0131–7310 (red square), the new pulsars, PSR J0043–73 (green square), and PSR J0052–72 (blue square).

4 RESULTS

We discovered two new pulsars, and identified 2 additional low signal to noise (S/N) candidates in our targeted survey of the SMC. We also detected the known PSR J0131–7310 (Manchester et al. 2006). We folded the raw data with `dspsr`, and then refined the periods, DMs and S/Ns with `pdmp`. The quoted values were obtained from `pdmp`, unless specified otherwise. Table 5 lists the pulsar properties and the PMB beam coordinates within which the pulsars were detected.

4.1 PSR J0131–7310

PSR J0131–7310 was detected in the 2017–08–25 pointing, focused on MCSNR J0127-7332. The pulsar was on the edge of one of the inner ring beams of the PMB (Figure 1, red square), with beam coordinates of RA = 01:32:46.87 and Dec = –73:16:21.80 (beam 5). We detected PSR J0131–7310 with a barycentric period of 348.12341 (18) ms, and a DM of 206.7 (1.5) pc cm^{-3}, matching well the Manchester et al. (2006) values for the period of 348.124045581 (7) ms and a DM of 205.2 pc cm^{-3}. PSR J0131–7310 was not detected in the second observation on 2017–09–11, but was detected again in the follow-up observation on 2017–12–13 with the `FFA`. Figure 3 shows the pulse profile of PSR J0131–7310 for the 2017–08–25 pointing.

4.2 PSR J0043–73

The first new SMC radio pulsar has a barycentric period of 937.42937 (26) ms and DM of 115.1 (3.4) pc cm^{-3}, which is consistent with the known SMC pulsar DM range (76 – 205 pc cm^{-3}). Hereafter the new pulsar will be referred to as PSR J0043–73 (Figure 1, green square). The pulsar was found in the 2017–08–25 pointing of which the XMMU J0049.0-7306 source was the focus, with beam coordinates of RA = 00:43:25.86 and Dec = –73:11:18.60 (beam 7), but not in the following observation on 2017-09-11. The pulsar was discovered using the FFA, but could clearly be seen in the `PRESTO prepfold` plot when folding the raw data with the identified period and DM. When we increased the

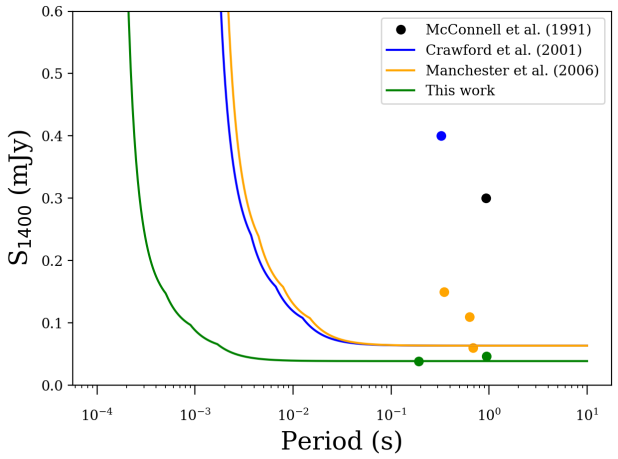

Figure 2. The 1400 MHz limiting flux densities for all SMC radio pulsar surveys. The filled circles represent the pulsars detected in the various surveys, in particular the green filled circles indicate the pulsars discovered in this survey (PSR J0043-73, PSR J0052–72).

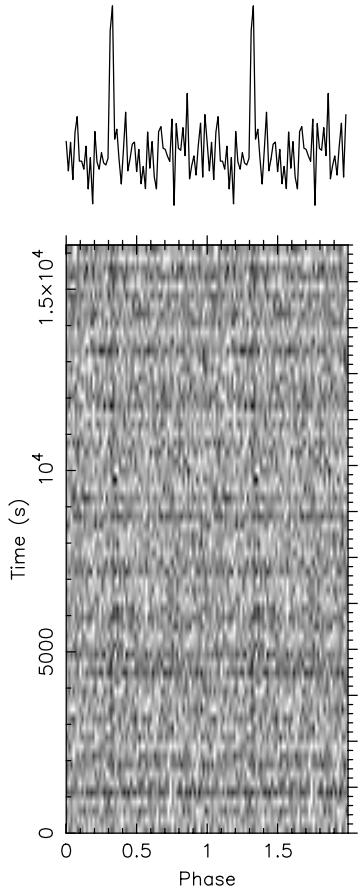

Figure 3. The integrated pulse profile (top panel) of PSR J0131–7310, as well as the pulse intensity as a function of pulse phase and integration time (grey scale). The pulses are plotted over two pulse phases.

number of summed harmonics to 16, `PRESTO` also identified PSR J0043–73 as a candidate pulsar. Figure 4 shows the FFA discovery plot. We used the archival Parkes data of the Manchester et al. (2006) survey, and used `prepfold` to fold the data at PSR J0043–73's period and DM, but did not recover the pulsar.

The known SMC pulsar, PSR J0045–7319 (Figure 1, black circle on left-hand corner edge of green square) has a similar period, but is located 33.24 arcmin from the centre of the beam within which PSR J0043–73 was found. This is nearly 5 times the HPBW radius, moreover PSR J0045–7319 has a period of 926.2 ms and a DM of 105.4 pc cm^{-3} (Crawford et al. 2001;Manchester et al. 2005[2]). Thus, we are confident that PSR J0043–73 is a new SMC radio pulsar.

4.3 PSR J0052–72

PSR J0052–72 (Figure 1, blue square) is the second new SMC pulsar (Figure 5) with a barycentric period of 191.444328 (46) ms and a DM of 158.6 (1.6) pc cm^{-3}. The pulsar was detected in one of the outer ring beams (beam 8) of the 2017–09–12 data set, which was focused on SNR C3. The beam (RA = 00:52:28.65, Dec = -72:05:13.5) was intersected by two inner ring beams from XMMU J0056.6-7208 and SNR C2, but PSR J0052–72 was not detected in either of the beams. The FFA was adapted to search for the pulsar's period, and subsequently detected the pulsar as well. PSR J0052–72 was re-detected in the 2017–08–28 dataset (beam 9) with the FFA. We also used the archival Parkes data of the Manchester et al. (2006) survey that was coincident with this pointing, and folded the data at the period and DM of PSR J0052–72, but the pulsar was not detected in the dataset.

4.4 Candidate Pulsars

We detected two lower S/N candidates, but could not confirm them. One of the candidates was detected in the 2017–09–12 dataset foucsed on SNR C3, and the other in the 2017–09–28 dataset focused on SNR C9. The SNR C3 candidate had a period and DM of 21.03561023 (40) ms and 208.42 pc cm^{-3} respectively, while the SNR C9 candidate had period of 11.001403386 (76) ms and a DM of 341.58 pc cm^{-3}. Both candidates were located in beam 5. We list the candidate pulsars in Table 5, and show the `prepfold` plots in Figure A1 and Figure A2.

5 DISCUSSION

Two new SMC radio pulsars were discovered in our SMC SNR survey, increasing the SMC pulsar population to seven confirmed pulsars. Furthermore, two candidates have been identified, but could not be confirmed. The detected and candidate pulsar properties are shown in Table 5.

[2] http://www.atnf.csiro.au/research/pulsar/psrcat/

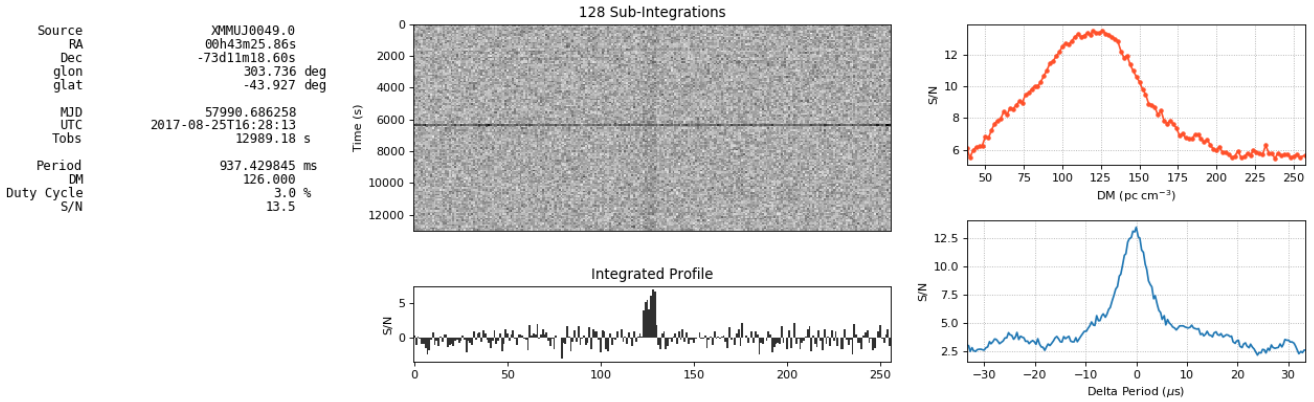

Figure 4. The FFA discovery plot of PSR J0043–73, which was located in beam seven of the XMMU J0049.0-7306 pointing on 2017–08–25. The bottom central panel show the integrated pulse profile. Following the discovery, we folded the raw data with `pdmp`, constraining the barycentric period to 937.42937 (26) ms and the DM to 115.1 (3.4) pc cm^{-3}. The pulsar was not detected in the initial young pulsar search with `PRESTO`.

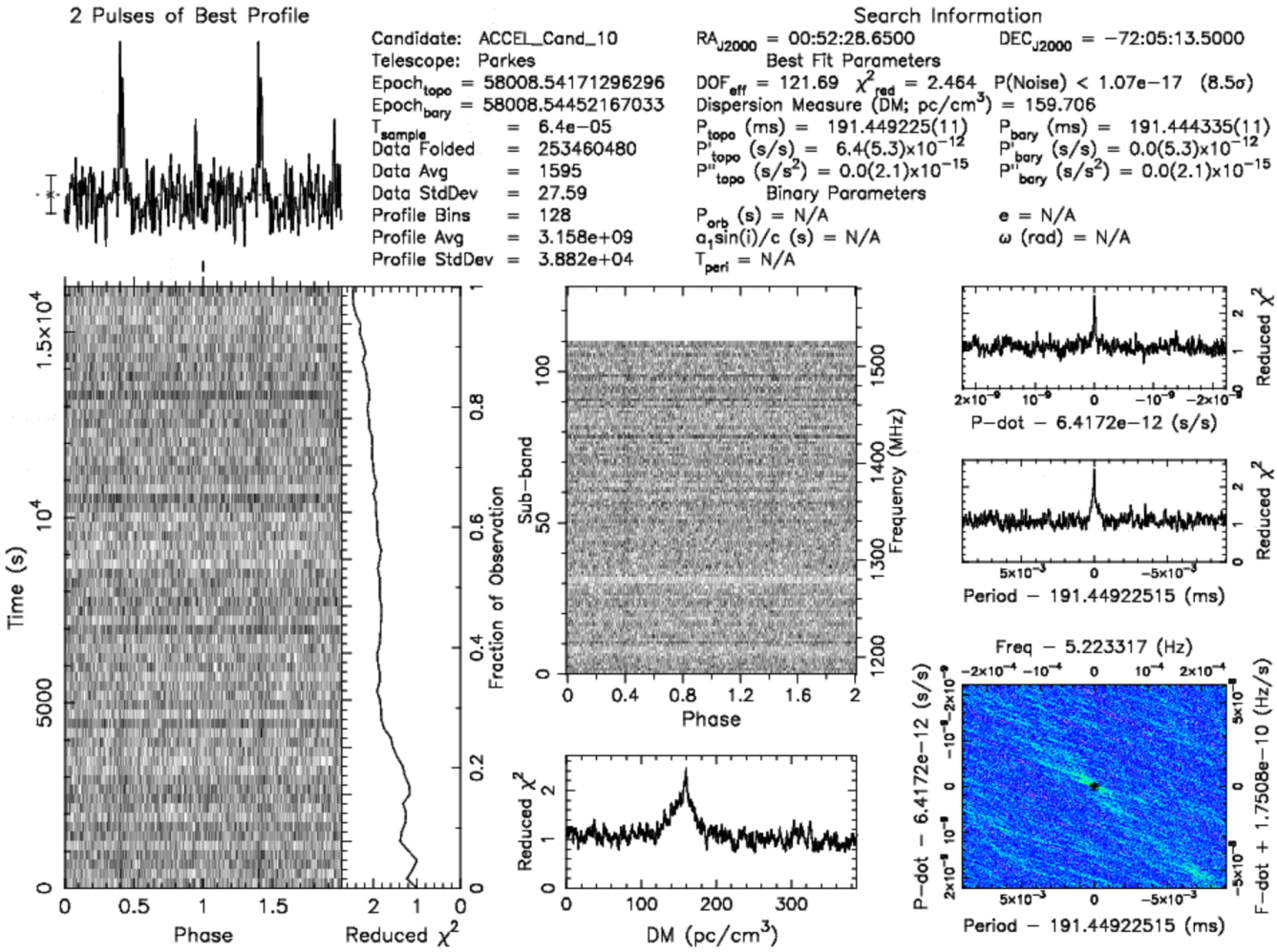

Figure 5. The `PRESTO` discovery plot of PSR J0052–72, which was located in beam eight of the SNR C3 pointing on 2017–09–12. PSR J0052–72 has a barycentric period to 191.444328 (46) ms and a DM of 158.6 (1.6) pc cm^{-3}.

Table 5. Properties of detected and candidate pulsars discovered in this survey.

JName	Date	Beam	Epoch[a] (J2000)	RA_{beam}[b] (J2000)	Dec_{beam}[b] (MJD)	P[c] (ms)	DM ($pc\,cm^{-3}$)	S_{1400} (mJy)	Method (PRESTO/FFA)
PSR J0131–7310	2017–08–25	5	57990.50	01 32 46.87	-73 16 21.80	348.12341 (18)	206.7 (1.5)	0.157	FFA
PSR J0043–73	2017–08–25	7	57990.69	00 43 25.86	-73 11 18.60	937.42937 (26)	115.1 (3.4)	0.047	FFA
PSR J0052–72	2017–09–12	8	58008.54	00 52 28.65	-72 05 13.50	191.444328 (46)	158.6 (1.6)	0.039	PRESTO
SNR C3 candidate	2017–09–12	5	58008.54	01 09 08.68	-72 16 34.10	21.0356101 (55)	208.17 (66)	0.038	PRESTO
SNR C9 candidate	2017–09–28	5	58024.71	01 10 15.74	-73 55 33.00	11.0014027 (11)	342.08 (32)	0.043	PRESTO

[a]Observation Epoch is taken to be at the start of a particular observation.
[b]The PMB coordinates within which a pulsar was detected.
[c] This period refers to the barycentric period.

Table 6. SMC pulsar parameters.

JName	P (ms)	DM ($pc\,cm^{-3}$)	S_{1400} (mJy)	Discovery Ref.
J0043–73	937.42937 (26)	115.1 (3.4)	0.047	1
J0045–7042	632.33580002 (6)	70 (3)	0.11	2
J0045–7319	926.27590497 (3)	105.4 (7)	0.3	4
J0052–72	191.444328 (46)	158.6 (1.6)	0.039	1
J0111–7131	688.54151164 (5)	76 (3)	0.06	2
J0113–7220	325.88301613 (1)	125.49 (3)	0.4	3
J0131–7310	348.124045581 (7)	205.2 (7)	0.15	2

Discovery references: (1) This work, (2) Manchester et al. (2006), (3) Crawford et al. (2001), (4) McConnell et al. (1991).

5.1 Detected pulsars

Our survey schedule enabled us to observe each target twice. In theory this would allow us to cross-match likely candidates, and so doing confirm candidates as pulsars when they are detected in both observations. We detected PSR J0052–72 in both pointings (2017–08–28 and 2017–09–12), however PSR J0043–73 was only detected in the first pointing on 2017–08–25. This was a result of more severe RFI, as well as rednoise during the second pointing on 2017–09–11. In particular, mitigating the rednoise effects for pulsars with periods greater than 200 ms is not a trivial task when a Fourier based pulsar search is implemented as shown by van Heerden et al. (2016). Thus, it is not suprising that we detected both pulsars, PSR J0131–7310 and PSR J0043–73, with the FFA and not initially in the Fourier based PRESTO search. Table 6 lists the properties of the now, seven SMC pulsars.

5.1.1 PSR J0131–7310

PSR J0131–7310 was detected at 20.55 arcmin from the centre of an inner ring beam, which was coincident with the first side lobe of beam five. Using the inner ring beam model of Ravi et al. (2016) we scaled the gain appropriately and calculated a flux density of 0.16 mJy for S/N = 11.90 and a pulse width of 4.20 ms. This is comparable to the 0.15 mJy flux density recorded for PSR J0131-7310 at 1400 MHz by Manchester et al. (2006).

5.1.2 PSR J0043–73

To calculate the flux density of PSR J0043–73 we used the radiometer equation with a S/N ratio of 18 and a pulse width of 25 ms, we determine $S_{1400} = 0.047$ mJy for an inner ring beam (Figure 2). We propose it as a new pulsar, in spite of a non-detection in the subsequent observation on 2017–09–11 when the data was compromised with severe RFI. This is also consistent with the non-detection of PSR J0131-7310 which was also observed on 2017–09–11.

5.1.3 PSR J0052–72

To calculate the flux density of PSR J0052–72 we used the radiometer equation with a S/N ratio of 11 and a pulse width of 8 ms, we determine $S_{1400} = 0.039$ mJy for an outer ring beam (Figure 2). This is the fastest spinning radio pulsar discovered in the SMC to date.

5.2 Non-detections

During this survey we observed 15 SNRs (candidates and confirmed), some of which are identified as PWNe. No pulsars were detected within any of these regions, but we can quantify flux density limits at a 8σ detection threshold for each of the sources, scaled by their distance from the centre of the beam in question (Table 7). We used the PMB beam model by Ravi et al. (2016) in combination with equation (1), and our survey parameters listed in Section 2.3, which we then multiplied by $\sqrt{\frac{W_{50}}{P-W_{50}}}$, and we set $W_{50} = 0.05P$.

5.2.1 SNR Candidates

Our deep, sensitive observations of MCSNR J0127-7332 and five SMC SNR candidates , identified by the XMM-Newton survey (Haberl et al. 2012), and optically selected by MCELS (Smith & MCELS Team 1999) and SALT Fabry-Perot observations, did not reveal any coincident radio pulsars. The size of each SNR candidate was less than the HPBW of the central PMB, thus the SNR candidates were each observed in their entirety in a single pointing. The sensitivity limit for each SNR candidate and MCSNR J0127-7332 is listed in the first six lines of Table 7.

Table 7. Properties of all SNRs/PWNe observed during our survey. The first six entries was the focus of our survey, which included the known SNR, MCSNR J0127-7332, and the five SNR candidates. The remaining SNRs/PWNe are listed in Filipović et al. (2008).

SNR	Pointing	RA_{SNR}[a] (J2000)	Dec_{SNR}[a] (J2000)	RA_{beam}[b] (J2000)	Dec_{beam}[b] (J2000)	D_{extent}[c] (arcmin)	d_{centre}[d] (arcmin)	S_{1400}[e] (mJy)	Type (SNR/PWN
MCSNR J0127-7332	MCSNR J0127-7332	01 27 45.95	-73 32 56.30	01 27 37.66	-73 35 20.50	-	3.17	0.024	SNR
XMMU J0049.0-7306	XMMU J0049.0-7306	00 49 46.00	-73 06 17.00	00 49 54.48	-73 04 09.70	0.75	2.21	0.027	SNR
SNR C3	SNR C3	01 03 35.56	-72 01 35.10	01 03 27.99	-72 03 41.30	1.38	2.18	0.024	SNR
SNR C2	SNR C2	00 56 25.00	-72 19 05.00	00 56 31.02	-72 15 48.40	3.72	3.31	0.026	SNR
XMMU J0056.6-7208	XMMU J0056.6-7208	00 56 26.00	-72 09 42.00	00 56 37.69	-72 09 01.40	4.02	1.12	0.024	SNR
SNR C9	SNR C9	01 12 37.00	-73 26 05.00	01 12 39.07	-73 28 15.40	5.85	2.18	0.025	SNR
DEM S5	XMMU J0049.0-7306	00 41 00.10	-73 36 30.00	00 41 24.24	-73 39 24.80	2.66	3.39	0.035	PWN
B0050-72.8	XMMU J0049.0-7306	00 52 36.90	-72 37 18.50	00 51 35.18	-72 36 02.30	2.41	4.79	0.042	SNR
IKT 16	SNR C3	00 58 17.80	-72 18 07.40	00 58 06.93	-72 19 17.60	3.32	1.43	0.036	PWN
IKT 21	SNR C3	01 03 17.00	-72 09 45.00	01 03 27.99	-72 03 41.30	1.20	6.12	0.026	SNR
1E0102-723	SNR C3	01 04 01.20	-72 01 52.30	01 03 27.99	-72 03 41.30	0.34	3.14	0.024	SNR
B0058-71.8	SNR C2	01 00 23.90	-71 33 41.10	01 00 19.47	-71 28 15.00	3.50	5.45	0.036	SNR
IKT 25	SNR C2	01 06 27.50	-72 05 34.50	01 07 23.94	-72 06 41.50	1.13	4.45	0.035	SNR
N S66D	XMMU J0056.6-7208	00 58 00.00	-72 11 01.40	00 56 37.69	-72 09 01.40	3.34	6.61	0.027	SNR
HFPK 334	XMMU J0056.6-7208	01 03 29.50	-72 47 23.20	01 04 25.17	-72 45 33.80	1.00	4.51	0.032	SNR

[a]The SNR coordinates.
[b]The PMB coordinates within which the SNR was located.
[c]D_{extent}: the angular extent of the SNR.
[d]d_{centre}: The distance from the centre of the SNR to the centre of the particular PMB beam.
[e]S_{1400}: The flux density values are calculated based on d_{centre} for $\sigma = 8$.

5.2.2 MCSNR J0127-7332 and SNR C3 Pointings

The MCSNR J0127-7332 and SNR C3 pointings were coincident with SXP 1062 and SXP 1323 respectively. Both these X-ray pulsars have extraordinarily long spin periods and are potentially associated with SNRs. In particular, NSs are typically born with spin periods of tens of milliseconds of (e.g. Crab and Vela pulsars), however Ikhsanov (2012) found that a young NS can possibly be spun down within 10^4 years by accreting matter from a magnetic wind, if the NS has a magnetic field of $\sim 10^{13}$ G. Alternatively, Fu & Li (2012) as well as Ho & Andersson (2017) showed that both accreting and isolated NSs with a $B > 10^{14}$ G (i.e. a magnetar) can spin down to $P > 1000$ s within the lifetime of a SNR.

I) MCSNR J0127-7332 Pointing

SXP 1062 is a transient Be\X-ray binary (BeXB) with an orbital period of 668 days, a lower limit eccentricity of 0.4, and a X-ray spin period of 1086 s (González-Galán et al. 2018). SXP 1062 has been spinning down from a period of 1062 s in 2010 to 1086 s in 2014. This is the second longest spin period known for a BeXB. If MCSNR J0127-7332 is the natal SNR of SXP 1062 it implies a kinematic age of $\sim$2-4$\times 10^4$ years for the NS (Hénault-Brunet et al. 2012). This contradicts standard models, which suggests that NSs at this age are too young to enter an accretion phase, and as a result cannot be X-ray pulsars (Lipunov 1992). SXP 1062 is in some aspects similar to the highly eccentric gamma-ray binary system PSR B1259–63, which has a young radio pulsar of $P \sim 47$ ms (Johnston et al. 1992) with a characteristic age of 3.32×10^5 years in orbit around a Be star. The system has a similarly long orbital period of 1236.7 days, and an eccentricity of 0.87 (Wang et al. 2004). We searched MCSNR J0127-7332 for radio pulsations at the X-ray spin period of SXP 1062, but did not detect any pulsations. The limiting flux density of this pointing was 0.024 mJy (Table 7).

II) SNR C3 Pointing

SXP 1323 is another peculiar BeXB with a 26.2 day orbital period, and a X-ray spin period of 1100 s (Carpano et al. 2017). SXP 1323 has the longest spin period known for any accreting X-ray pulsar, but has been rapidly spun up in a period between 2006 and 2016 from 1340 s to 1100 s. Recently, Gvaramadze et al. (2019) found evidence for a putative SNR centred on SXP 1323. They identified the SNR with optical studies, however it is the same SNR discovered by XMM-Newton and referred to as SNR C3 in this paper. If the SNR is associated with SXP 1323 then the NS's age is estimated to be 4×10^4 years, similar to SXP 1062's age. This would be the second, long period X-ray pulsar located in its natal SNR, and interestingly both are hosted in the low metallicity environment of the SMC. However, SXP 1323 has a much shorter orbital period than SXP 1062, and subsequently could accrete matter more often. Accretion typically inhibits radio pulsations, and indeed we did not detect any radio pulsations at the X-ray spin period.

Furthermore, the SNR C3 pointing included 2 confirmed SNRs (1E0102-723, IKT 21) in the central beam, as well as IKT 16 in the second beam. 1E0102-723 was first detected in the X-rays by Seward & Mitchell (1981), and then identified by Dopita et al. (1981) as an oxygen rich SNR with narrow band optical imaging. In a subsequent study, Vogt et al. (2018) identified an isolated neutron star with characteristics consistent with a central compact object (CCO). From their study the CCO is likely associated with 1E0102-723, thus one would not expect to dectect radio pulsations

from 1E0102-723, since CCOs are radio quiet. Conversely, IKT 16 has been confirmed as a PWN with a hard X-ray point source (Maitra et al. 2015). In particular, the X-ray spectral index of 1.1 implies that the emission is dominated by non-thermal emission originating from a pulsar. The expected spin down power of 10^{37} erg s^{-1} suggests the existence of a ∼100 ms pulsar. Down to the 1400 MHz flux limit of 0.024 mJy we did not detect any pulsations, thus the pulsar must be either too faint or not beaming towards us.

A pulsar BeXB system, SAX J0103-722 with a X-ray spin period of 345 s (Hughes & Smith 1994; Israel et al. 2000; van der Heyden et al. 2004), is coincident with IKT 21. However, it is not clear whether SAX J0103-722 is associated with IKT 21 or merely a chance coincidence. Hughes & Smith (1994) argued that a spatial chance coincidence in the SMC is highly unlikely, and would require a transverse spatial velocity exceeding 100 km s^{-1} if the NS of SAX J0103-722 was born by the same supernova explosion that resulted in the formation of IKT 21. Such a large spatial velocity for a BeXB is improbable. Instead, the study suggests the SN explosion occurred in an OB association which also harbours SAX J0103-722. Nonetheless, we did not detect any radio pulsars down to a flux limit of 0.026 mJy.

5.2.3 XMMU J0049.0-7306 Pointing

The XMMU J0049.0-7306 pointing included DEM S5 and B0050–72.8 (Table 7). The nature of the compact object originating from the precursor SN explosion is not known for B0050–72.8, nor has any candidates been identified. We did not detect any radio pulsations down to a sensitivity of of 0.042 mJy. Alasberi et al. 2019 (in prep) has confirmed DEM S5 as a PWN, with a morphological structure analogous to PSR B1951+32 in SNR CTB 80 (Safi-Harb et al. 1995) and 'the mouse' (Camilo et al. 2002). Although this discovery confirms the likely existence of a radio pulsar, we did not detect any radio pulsations down to a flux density of 0.035 mJy.

5.2.4 SNR C2 Pointing

The SNR C2 pointing included B0058-71.8 and IKT 25 in the outer ring beams of the PMB (Table 7). B0058-71.8 has not been studied in detail, and we did not detect any radio pulsations at a flux limit of 0.036 mJy. Conversely, IKT 25 was likely produced by a thermonuclear (Type Ia) supernova (Roper et al. 2015; Lee et al. 2011), thus one would not expect a NS to form, and thus one would not expect a radio pulsar residing in the SNR, and indeed we did not detect radio pulsations down to a sensitivity of 0.035 mJy.

5.2.5 XMMU J0056.6-7208 Pointing

N S66D was located on the edge of the central beam during the XMMU J0056.6-7208 pointing, while HFPK 334 was positioned in one of the outer ring beams of the PMB. N S66D is poorly studied, consequently no additional information is available in the literature. On the contrary HFPK 334 is a young ($\leqslant$ 1800 years) (Crawford et al. 2014), intriguing SNR emitting X-ray and radio emission, but not detectable in the optical (Payne et al. 2007). Filipović et al. (2008) noted a central point source within HFPK 334, and suggested that it may be indicative of a PWN. In light of their study Crawford et al. (2014) conducted a X-ray study of the central object, but could not identify it as either a CCO or a pulsar, thereupon they proposed that the central point source is a background object. The lack of any radio pulsations in our study down to a flux limit of 0.032 mJy, supports their theory that the central source is a background object.

6 CONCLUSIONS

We report the first pulsar discoveries in the SMC since the Manchester et al. (2006) survey. We discovered PSR J0043–73, a 937.42937 ms pulsar with DM = 115.1 pc cm^{-3}, as well as the fastest spinning pulsar to date in the SMC, PSR J0052–72 with P = 191.444328 ms and DM = 158.6 pc cm^{-3}. These discoveries increases the SMC radio pulsar population to seven, corresponding to a 40% increase in the population. To date no radio pulsar SNR association has been made in the SMC.

ACKNOWLEDGEMENTS

The Parkes radio telescope is part of the Australia Telescope which is funded by the Commonwealth of Australia for operation as a National Facility managed by CSIRO. NT, VMc, and DAHB acknowledges support of the National Research Foundation of South Africa (grants 98969, 93405, and 96094). BWS, VM and MC acknowledge funding from the European Research Council (ERC) under the European Union's Horizon 2020 research and innovation programme (grant agreement No. 694745).

REFERENCES

Antoniou V., Zezas A., 2016, MNRAS, 44, 1
Badenes C., Maoz D., Draine B. T., 2010, MNRAS, 407, 1301
Camilo F., 2003, ASPS, 302, 145,150
Camilo F., Manchester R. N., Gaensler B. M., Lorimer D. R., 2002, ApJ, 579, L25
Carpano S., Haberl F., Sturm R., 2017, A&A, 602, A81
Crawford E. J., Filipović M. D., McEntaffer R. L., Brantseg T., Heitritter K., Roper Q., Haberl F., Urosević D., 2014, AJ, 148
Crawford F., Kaspi V. M., Manchester R. N., Lyne A. G., Camilo F., D'Amico N., 2001, ApJ, 553, 367
Dickey J. M., Lockman F. J., 1990, ARA&A, 28, 215
Dopita M. A., Tuohy I. R., Mathewson D. S., 1981, ApJ, 248, L105
Filipović M. D. et al., 2008, A&A, 485, 63
Filipović M. D., Payne J. L., Reid W., Danforth C. W., Staveley-Smith L., Jones P. A., White G. L., 2005, MNRAS, 364, 217
Fu L., Li X.-D., 2012, ApJ, 757, 171
González-Galán A., Oskinova L. M., Popov S. B., Haberl F., Kühnel M., Gallagher J., Schurch M. P. E., Guerrero M. A., 2018, MNRAS, 475, 2809
Gorham P. W., Ray P. S., Anderson S. B., Kulkarni S. R., Prince T. A., 1996, ApJ, 458, 257

Green D. A., 2014, BASI, 42, 47
Gvaramadze V. V., Kniazev A. Y., Oskinova L. M., 2019, MNRAS, 485, L6
Haberl F., Sturm R., 2015, A&A, 81, 17
Haberl F. et al., 2012, A&A, 545, A128
Hénault-Brunet V. et al., 2012, MNRAS, 420, L13
Ho W. C. G., Andersson N., 2017, MNRAS, 464, L65
Hughes J. P., Smith R. C., 1994, AJ, 107, 1363
Ikhsanov N. R., 2012, MNRAS, 424, L39
Israel G. L. et al., 2000, ApJ, 531, L131
Johnston S., Manchester R. N., Lyne A. G., Bailes M., Kaspi V. M., D'amico N., 1992, ApJ, 387, 37
Kaspi V. M., Johnston S., Bell J. F., Manchester R. N., Bailes M., Bessell M., Lyne A. G., D'Amico N., 1994, ApJ, 423, 44
Kaspi, V. M., Helfand D. J., 2002, ASPCS, 271
Keane E. F., Kramer M., 2008, MNRAS, 391, 2009
Keith M. J. et al., 2010, MNRAS, 409, 619
Lee J.-J., Park S., Hughes J. P., Slane P. O., Burrows D. N., 2011, ApJ, 731, L8
Lipunov V. M., 1992, Astrophysics of Neutron Stars
Lorimer D. R., Lyne a. G., Camilo F., 2000, ASPC, 221, 83
McConnell D., McCulloch P. M., Hamilton P. A., Ables J. G., Hall P. J., Jacka C. E., Hunt A. J., 1991, MNRAS, 249, 654
McMahon P., 2008, Msc., University of Cape Town
Maitra C., Ballet J., Filipović M. D., Haberl F., Tiengo A., Grieve K., Roper Q., 2015, A&A, 584, A41
Manchester R. N., Fan G., Lyne A. G., Kaspi V. M., Crawford F., 2006, ApJ, 649, 235
Manchester R. N., Hobbs G. B., Teoh A., Hobbs M., 2005, VizieR Online Data Catalog, 7245
Manchester R. N. et al., 2001, MNRAS, 328, 17
Payne J. L., White G. L., Filipović M. D., Pannuti T. G., 2007, MNRAS, 376, 1793
Ransom S. M., Eikenberry S. S., Middleditch J., 2002, ApJ, 124, 1788
Ravi V. et al., 2016, Science, 354, 1249
Ridley J. P., Crawford F., Lorimer D. R., Bailey S. R., Madden J. H., Anella R., Chennamangalam J., 2013, MNRAS, 433, 138
Roper Q., McEntaffer R. L., DeRoo C., Filipovic M., Wong G. F., Crawford E. J., 2015, ApJ, 803, 106
Safi-Harb S., Ogelman H., Finley J. P., 1995, ApJ, 439, 722
Seward F. D., Mitchell M., 1981, ApJ, 243, 736
Smith R. C., MCELS Team 1999, in Chu Y.-H., Suntzeff N., Hesser J., Bohlender D., eds, IAU Symposium Vol. 190, New Views of the Magellanic Clouds. p. 28
Staelin D. H., 1969, in IEEE Proceedings. p. 724
Stanimirovic S., Dickey J. M., Sault R. J., Snowden S. L., 1999, MNRAS, 436, 417
Staveley-Smith L. et al., 1996, PASA, 13, 243
Sturm R. et al., 2013, A&A, 558, A3
van der Heyden K. J., Bleeker J. A. M., Kaastra J. S., 2004, A&A, 421, 1031
van Heerden E., Karastergiou A., Roberts S. J., 2016, MNRAS, 467, 1661
Vogt F. P. A., Bartlett E. S., Seitenzahl I. R., Dopita M. A., Ghavamian P., Ruiter A. J., Terry J. P., 2018, Nature Astronomy, 2, 465
Wang N., Johnston S., Manchester R. N., 2004, MNRAS, 351, 599

APPENDIX A: PULSAR CANDIDATES

Here follows the `prepfold` plots for two pulsar candidates found during the young pulsar search with `PRESTO`.

This paper has been typeset from a TEX/ LATEX file prepared by the author.

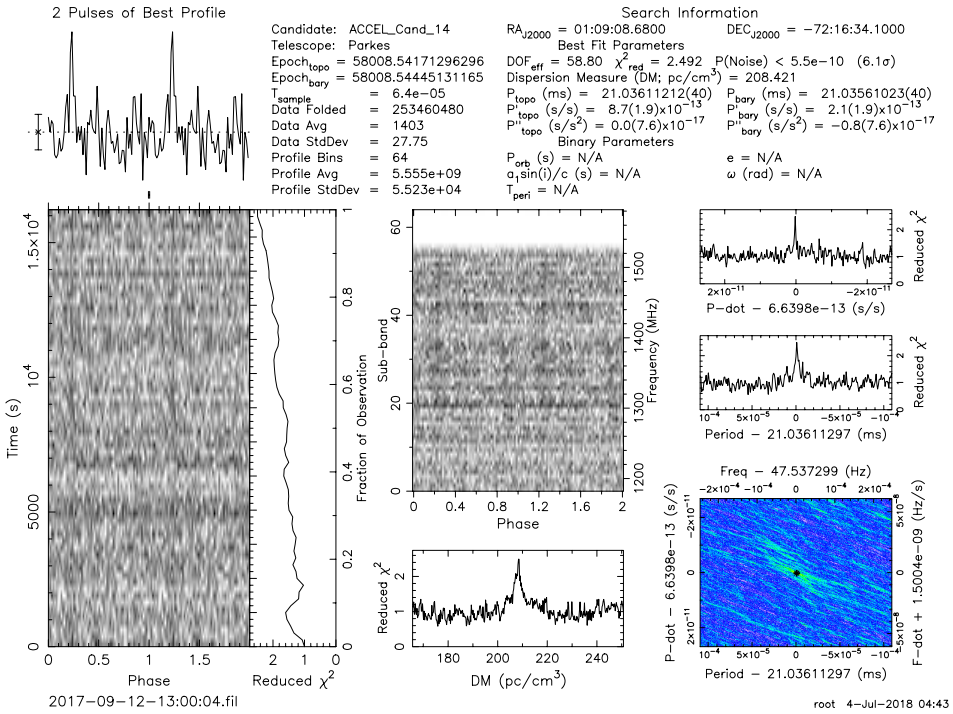

Figure A1. This candidate was detected during a SNR C3 pointing on 2017–09–12. The candidate was located in beam five.

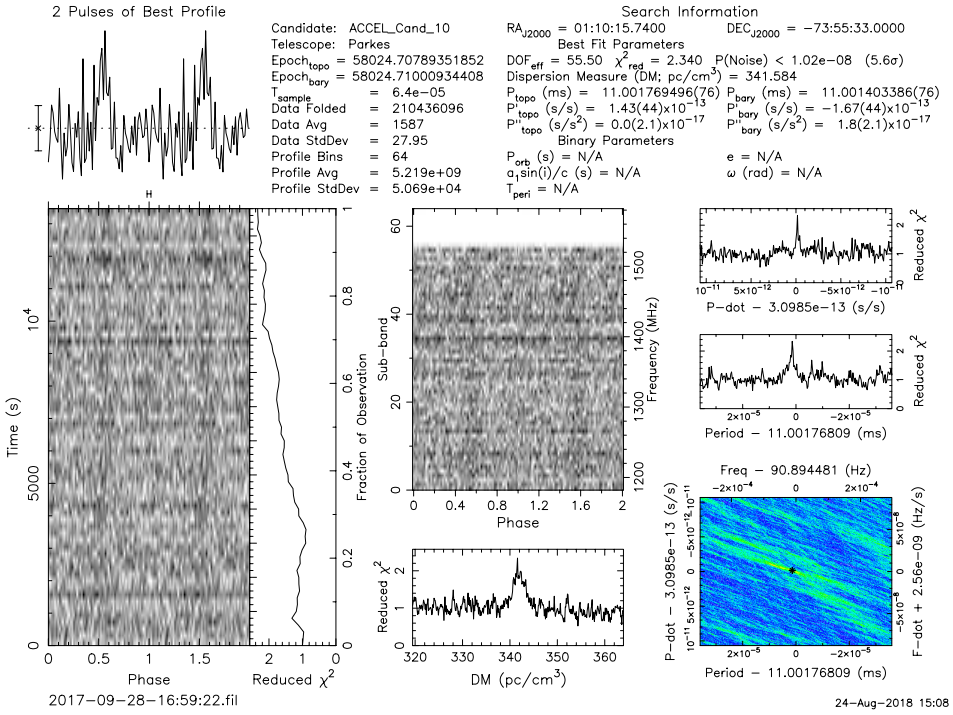

Figure A2. This candidate was detected during a SNR C9 pointing on 2017–09–28. The candidate was found in beam five.